

## Effect of Structural Defects and Impurities on the Excited State Dynamics of 2D BA<sub>2</sub>PbI<sub>4</sub> Perovskite

Gélvez-Rueda, María C.; Peeters, Sicco; Wang, Peng Cheng; Felter, Kevin M.; Grozema, Ferdinand C.

**DOI**

[10.1002/hlca.202000121](https://doi.org/10.1002/hlca.202000121)

**Publication date**

2020

**Document Version**

Final published version

**Published in**

Helvetica Chimica Acta

**Citation (APA)**

Gélvez-Rueda, M. C., Peeters, S., Wang, P. C., Felter, K. M., & Grozema, F. C. (2020). Effect of Structural Defects and Impurities on the Excited State Dynamics of 2D BA<sub>2</sub>PbI<sub>4</sub> Perovskite. *Helvetica Chimica Acta*, 103(9), Article e2000121. <https://doi.org/10.1002/hlca.202000121>

**Important note**

To cite this publication, please use the final published version (if applicable). Please check the document version above.

**Copyright**

Other than for strictly personal use, it is not permitted to download, forward or distribute the text or part of it, without the consent of the author(s) and/or copyright holder(s), unless the work is under an open content license such as Creative Commons.

**Takedown policy**

Please contact us and provide details if you believe this document breaches copyrights. We will remove access to the work immediately and investigate your claim.

# Effect of Structural Defects and Impurities on the Excited State Dynamics of 2D BA<sub>2</sub>PbI<sub>4</sub> Perovskite

María C. Gélvez-Rueda,<sup>\*a</sup> Sicco Peeters,<sup>a</sup> Peng-Cheng Wang,<sup>a</sup> Kevin M. Felter,<sup>a</sup> and Ferdinand C. Grozema<sup>a</sup>

<sup>a</sup> Department of Chemical Engineering, Delft University of Technology, Van der Maasweg 9, NL-2629 HZ, Delft, The Netherlands, e-mail: m.c.gelvezrueda@tudelft.nl

Dedicated to Prof. *Michael Graetzel* on the occasion of his 75th birthday

© 2020 The Authors. Helvetica Chimica Acta Published by Wiley-VHCA AG. This is an open access article under the terms of the Creative Commons Attribution License, which permits use, distribution and reproduction in any medium, provided the original work is properly cited.

In this work, we show that the quality of the precursor and the thin film preparation strongly affect the optoelectronic properties of the 2D perovskite BA<sub>2</sub>PbI<sub>4</sub>. 2D perovskites with alkylammonium organic cations such as butylammonium (BA) are relatively soft structures that exhibit large dynamic disorder and phase variations. Here we show, by a variety of spectroscopy techniques (steady state absorption, photoluminescence and ultrafast transient absorption), that at temperatures below the phase transition (253 K) the material exhibits excitonic features from the room temperature phase (due to incomplete structural transition) and a broadband emission at 560–600 nm (due to self-trapped excitons) with varied relative intensities depending on the precursors and processing conditions. This suggests that the processing conditions have a large influence on the crystallization and introduction of extrinsic defect impurities directly affecting the optoelectronic properties. Making absolute statements about the properties of BA<sub>2</sub>PbI<sub>4</sub> requires improved control over the materials thin film deposition and a better understanding of the role of the lattice vibrational dynamics and extrinsic defects on the exciton dynamics.

**Keywords:** 2D perovskites, femtosecond transient absorption, photoluminescence, phase transitions, thin films.

## Introduction

Two-dimensional (2D) organic-inorganic lead halide perovskites are rapidly attracting research interest due to their promising efficiency in solar cells and their improved moisture stability, as compared to their 3D counterparts. In addition, they exhibit intriguing optoelectronic properties that make them suitable for other applications, for instance light emitting devices (LED), nano-lasers, photodetectors.<sup>[1–9]</sup> 2D Perovskites are layered analogues of 3D hybrid halide perovskites that are formed by partially or fully replacing the commonly used methylammonium (MA) cation with a larger alkylammonium (for instance butylammonium

(BA) or phenyl-alkylammonium (PEA)) cation. This reduces the general three-dimensional (3D) perovskite framework into a layered structure with inorganic octahedral lead-halide layers separated by the large organic cations.<sup>[10]</sup> In such structures, electrons and holes are dimensionally and dielectrically confined to the inorganic layer where they experience a large mutual attraction, resulting in stable excitons at room temperature with exciton binding energies ( $E_b$ ) of ~200 to 400 meV.<sup>[11,12]</sup> Despite the large exciton binding energies 2D perovskites with only one inorganic layer ( $n=1$ ), such as BA<sub>2</sub>PbI<sub>4</sub> with  $E_b = \sim 370$  meV,<sup>[13]</sup> generally exhibit inefficient photoluminescence. This low efficiency has been attributed to thermal quenching of the excitons or strong exciton-phonon interactions caused by lattice fluctuations and dynamic disorder.<sup>[4,12,14–19]</sup> The most widely studied 2D perovskites for device applications contain butyl-

Supporting information for this article is available on the WWW under <https://doi.org/10.1002/hlca.202000121>

ammonium (BA) mixed with MA to form multiple inorganic octahedral layers,  $\text{BA}_2\text{MA}_{n-1}\text{Pb}_n\text{I}_{3n+1}$  ( $n=2, 3, 4$ ). These multilayer, so-called 2D-3D 'Ruddlesden-Popper' phases have been used to make efficient solar cells and light-emitting diodes.<sup>[3,4]</sup> The efficiency of these devices improves with the number of layers as the confinement and exciton binding energy decrease, resulting in optoelectronic properties that are more similar to 3D perovskites and possibly due to an increased rigidity of the lattice.<sup>[8,9,13]</sup>

2D Perovskites with alkylammonium chains as organic compounds are relatively soft materials that exhibit considerable structural fluctuations due to low interaction between the chains, which ultimately leads to phase transitions close to room temperature.<sup>[20]</sup>  $\text{BA}_2\text{PbI}_4$  exhibits a phase transition (at  $\sim 253$  K) due to a reorientation of the BA cations, increasing the inorganic lattice distortion and band gap of the material from  $\sim 2.4$  eV to 2.56 eV.<sup>[20]</sup> In literature, there is no clear understanding of the relation between the excited state dynamics, the nature of the organic cation and thermal lattice fluctuations (phonon vibration modes) in 2D perovskites.<sup>[21,22]</sup> Some studies have reported complex absorption and emission spectra (many transitions energies) at low temperatures of which the origin has been related to several effects such as phase transitions, strong many-body interactions between the excitons in the inorganic layer and/or formation of higher order biexcitons and self-trapped excitons.<sup>[12,23–31]</sup> A comparison of all these studies reveals that there are large differences in the relative intensities of the different features in the spectra, especially in the broad band emission intensities at  $\sim 560$ – $800$  nm that are associated with self-trapped excitons.<sup>[26–30]</sup> Studies to design broadly emitting perovskite compounds associate efficient self-trapped exciton emission from lattice distortions of the inorganic cages.<sup>[26–30]</sup> However, the large differences in the relative intensities point to self-trapped excitons in defects introduced during the preparation methods.<sup>[26]</sup> This suggests that the quality and preparation methods of 2D perovskites are critical to understand the complexities in the observed excited state dynamics.

In this work, we have studied the excited state dynamics of  $\text{BA}_2\text{PbI}_4$  thin films obtained by different preparation methods with a variety of spectroscopy techniques (steady state absorption, photoluminescence and ultrafast transient absorption) as a function of temperature. We have found that the initial quality of the precursor and the thin film preparation conditions strongly affect the optoelectronic proper-

ties. First, we have found that the use of  $\text{BA}_2\text{PbI}_4$  with a lower crystal quality (nanometer-micrometer powders) and unoptimized processing conditions (old solutions, higher processing temperatures, longer annealing time) results in higher emission intensities at 560–700 nm. This shows that broadband emission in 2D perovskites from self-trapped excitons is influenced by extrinsic defect impurities and not only by the lattice deformation. The emission from these defect states becomes larger at lower temperatures and exhibit a longer recombination lifetime than the excitonic transitions. In addition, we found that even in films prepared with the highest  $\text{BA}_2\text{PbI}_4$  quality (millimeter-size single crystals) processed under exactly the same conditions, the relative absorption or photoluminescence emission intensities from the excitonic states of the different phases at temperatures below the 253 K phase transition vary from sample to sample. This inhomogeneity shows that in  $\text{BA}_2\text{PbI}_4$  films, the phase transition is not complete below 253 K and control over these micro grains on thin films is very difficult. By performing ultrafast pump-probe transient absorption measurements as a function of temperature, we confirm the variability of relative intensities between the high and low temperature excitonic phases. This variability is related to the lack of interaction between the alkylammonium chains and the relative 'softness' of 2D perovskite structures with alkylammonium chains, leading to larger dynamic disorder and variations in the optoelectronic properties. This research shows that making absolute statements about the optoelectronic properties and excited state dynamics of 2D perovskites with alkylammonium molecules requires improved control over the materials thin film deposition and a better understanding of the role of the lattice vibrational dynamics and extrinsic defects on the exciton dynamics.

## Results and Discussion

### *Optoelectronic Properties of $\text{BA}_2\text{PbI}_4$*

In order to study the optoelectronic properties of  $\text{BA}_2\text{PbI}_4$ , we prepared thin films by hot-casting, varying the initial quality of the  $\text{BA}_2\text{PbI}_4$  crystals, temperature and spin-coating time. We used the hot-casting method, as it has been shown to yield the best quality of films for device applications.<sup>[9]</sup> First, we prepared  $\text{BA}_2\text{PbI}_4$  crystals by dissolving butylammonium (BA) molecules and  $\text{PbI}_2$  in stoichiometric amounts in HI at  $70^\circ\text{C}$  and precipitating them by cooling back to room temperature.<sup>[2]</sup> Depending on the cooling ramp and

precipitation time, it is possible to prepare millimeter-size single crystals or powders with nanometer to micrometer size domains (see details in the *Experimental Section*).<sup>[2]</sup> All depositions were started from fully synthesized  $\text{BA}_2\text{PbI}_4$  crystals in order to minimize the effect of the precursor ratios on the thin film preparation.<sup>[26–28]</sup> Subsequently, solutions of  $\text{BA}_2\text{PbI}_4$  were prepared by dissolving the synthesized single crystals or powders in dimethylformamide (DMF) at 343 K under magnetic stirring for 2 h. The fresh solutions were spin-coated on hot quartz substrates at 433 K, with a ramp of for 30 s and post-annealed for 15 min. We optimized the spin-coating conditions in order to obtain the best quality thin films. As it will be shown below, the conditions for crystal synthesis and spin-coating turn out to be critical for the optoelectronic properties and the presence of defects in  $\text{BA}_2\text{PbI}_4$ .

In *Figure 1,a* and *1,b* the X-ray diffraction (XRD) patterns of  $\text{BA}_2\text{PbI}_4$  single crystals, powders and thin films (TF) prepared from single crystals (TF–C) or from powders (TF–P) are shown. The synthesized single crystals and powders exhibit the main peaks from the simulated XRD obtained from the  $\text{BA}_2\text{PbI}_4$  crystal structure oriented in the (0 0 *l*) direction. Similarly, the thin films made from either crystals (TF–C) or powders (TF–P) also exhibit the (0 0 *l*) reflections characteristic of a preferential growth along the (1 1 0) direction parallel to the substrate.<sup>[1]</sup> From the perspective of the XRD measurements,  $\text{BA}_2\text{PbI}_4$  films have been prepared, and there is no difference between using millimeter size single crystals or powders as the starting material. Nevertheless, it is shown in *Figure 1,c* that films deposited with non-optimized spin-coating conditions (for example, use of old solutions, higher than 433 K temperatures or longer than 15 min annealing time)

can result in films with an additional XRD peak at  $\sim 5.2$   $2\theta$  (using a Co source). The origin of this peak is not clear, but as will be shown below it is directly linked to differences in absorption spectra and a larger broadband emission intensity at  $\sim 560$  nm to 600 nm.

In order to study the optoelectronic properties as a function of temperature, the transmission and photoluminescence spectra of the thin films were measured in a spectroscopy set up coupled to a helium cryostat. Inside the cryostat, it is only possible to measure the change in transmission of the materials, because multiple reflections on the windows in the cryostat cannot be corrected for. In *Figure 2*, the steady-state transmission and photoluminescence of  $\text{BA}_2\text{PbI}_4$  films are shown. In *Figure 2,a* and *2,c*, the transmission spectra at room temperature of  $\text{BA}_2\text{PbI}_4$  films made starting from single crystals and powders exhibit the typical features of 2D perovskites: an excitonic peak at  $\sim 510$  nm with a continuum step-like band absorption at shorter wavelengths ( $\sim 400$  nm), which is attributed to the free electron-hole transition.<sup>[1,2,32]</sup> It is worth highlighting that the transmission spectra of films based of nanocrystalline powders as a starting material are slightly blue-shifted compared to those based on single crystals and to spectra reported in literature.<sup>[1,2]</sup> In *Figure 2,e*, the non-optimized films exhibit an additional absorption feature at  $\sim 560$ –600 nm. The exact origin of this peak is not clear, but the comparison between the thin films based on the crystals, powder and unoptimized process conditions (*Figure 2,e*) suggests is extrinsic effect caused by impurities. When the temperature is decreased, the main absorption peak of all  $\text{BA}_2\text{PbI}_4$  films shifts from  $\sim 510$  nm at 294 K to  $\sim 484$  nm below 253 K. This shift is associated with a phase transition (occurring between 280 K and 260 K) caused by reorientation of the BA in between the

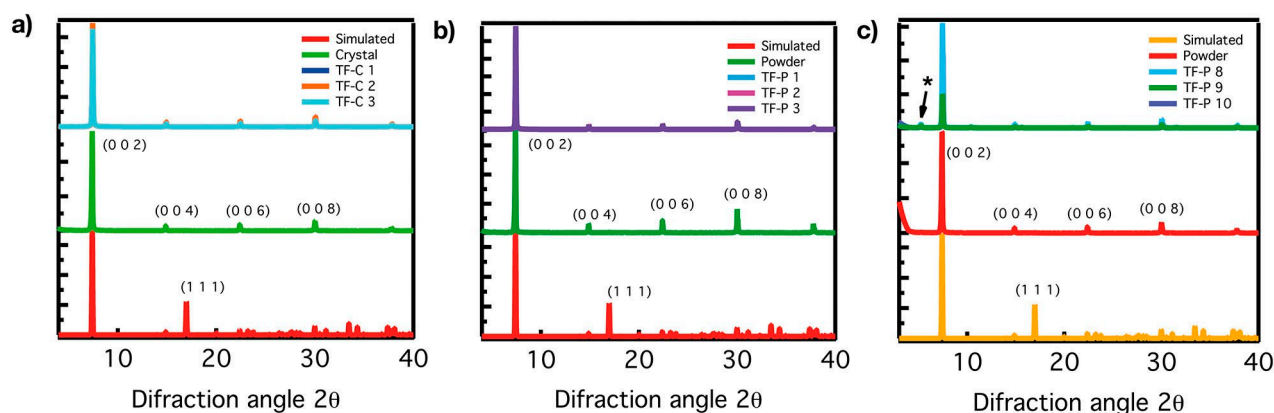


**Figure 1.** X-Ray diffraction of  $\text{BA}_2\text{PbI}_4$ . a)  $\text{BA}_2\text{PbI}_4$  Crystal and films prepared from crystals. b)  $\text{BA}_2\text{PbI}_4$  Powder and thin films prepared from powders. c)  $\text{BA}_2\text{PbI}_4$  Powder and unoptimized thin films prepared from powders.

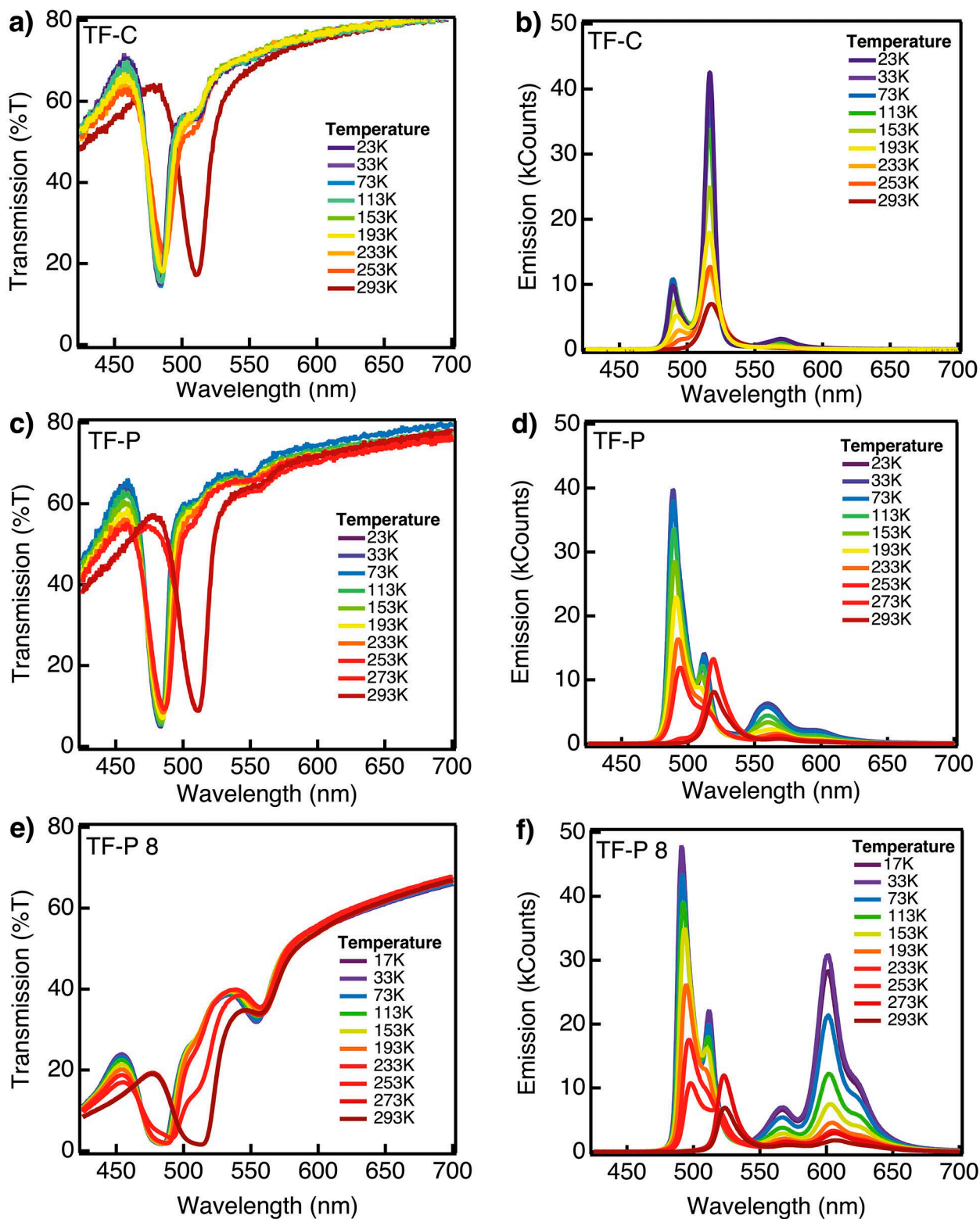


**Figure 2.** Temperature-dependent steady-state absorption and photoluminescence emission measured inside a Helium cryostat of  $\text{BA}_2\text{PbI}_4$ . a), b) Films from  $\text{BA}_2\text{PbI}_4$  crystalline precursors. c), d) Films from  $\text{BA}_2\text{PbI}_4$  powder precursors. e), f) Non-optimized films from  $\text{BA}_2\text{PbI}_4$  powder precursors. Photoluminescence excitation at 405 nm with a photon intensity  $\sim 1.7 \times 10^{17}$  photon/(s  $\text{cm}^2$ ).

inorganic octahedral layers.<sup>[20]</sup> This reorientation increases the distortion of the inorganic octahedral layers (increased corrugation) resulting in an increase of the band gap.<sup>[20,32]</sup> At temperatures below the phase transition (253 K), the transmission spectra of all  $\text{BA}_2\text{PbI}_4$  films still exhibit a shoulder at the position of the room temperature peak ( $\sim 510$  nm). This indicates that the phase transition to the low temperature phase (phase II) is not complete, and there is partial presence of the room temperature phase (phase I).<sup>[20,32]</sup> The absorption relative intensities of the different phases in the film, phase II at  $\sim 484$  nm and phase I at  $\sim 510$  nm, vary from sample to sample.

The photoluminescence emission spectra of  $\text{BA}_2\text{PbI}_4$  films are shown for different temperatures in *Figure 3,b* and *3,d*. In general, the photoluminescence intensity increases at low temperature due to more efficient radiative recombination of excitons (less thermal energy to dissociate).<sup>[13]</sup> At room temperature, the emission spectrum of  $\text{BA}_2\text{PbI}_4$  films exhibits a single emission peak ( $\sim 516$  nm) corresponding to the main exciton absorption peak ( $\sim 510$  nm). Once again, for the non-optimized film shown in *Figure 3,f*, there is an additional photoluminescence feature at  $\sim 600$  nm corresponding to the peak at 560 nm. For the optimized  $\text{BA}_2\text{PbI}_4$  films made from crystalline and powder precursor materials, lowering the temperature results in the appearance of the low energy peak at 489 nm due to the phase transition at 253 K, while the peak near 510 nm remains. In addition, below 200 K, weak emission features appear between 560 and 600 nm. These low wavelength emission peaks have a longer lifetime ( $\sim 3$ – $5$  ns) than the common exciton emission ( $\sim 490$  nm and 516 nm) in 2D perovskites ( $\sim 1$ – $2$  ns) (see *Figure S1* in *Supporting Information*) and are attributed in the literature to broadband emission from self-trapped excitons due to strong phonon-coupling with the distorted soft crystal structure and/or in extrinsic defect states.<sup>[26–30,33]</sup> The intensity of the broad-band emission features (and hence the concentration of self-trapped excitons in defects) is higher for the films prepared from  $\text{BA}_2\text{PbI}_4$  amorphous powders and non-optimized films than for the ones prepared from  $\text{BA}_2\text{PbI}_4$  single crystals (see *Figure 3,b*, *3,d* and *3,f*). These defects, and subsequent changes in photoluminescence spectra and dynamics, are associated to slight differences in stoichiometry and dynamic behavior of ions, particularly the diffusion of halides ions due to vacancies or interstitial defects.<sup>[26]</sup> To clarify the microstructure from the different samples, atomic force microscopy (AFM) measurements were performed on the thin films, see *Figure S2* in *Supporting Informa-*

*tion*. In *Figure S2*, it is clear that the size of the grains in the thin films prepared from crystals are larger ( $\sim 600$  nm) than in those prepared from powder precursor ( $\sim 100$  nm). As a result, the thin films prepared from powder precursors exhibit more surface defects that reflect in the presence of low energy emission peaks. As expected, the impact from defects becomes more evident at low temperature, as there is less thermal energy available to escape from the in-gap defect states. These results clearly show that the broad emission band exhibits a large variation per sample preparation and cannot be fully attributed to intrinsic self-trapped excitons due to strong phonon-coupling to the lattice distortions.<sup>[26]</sup> This defect-governed luminescence strongly resembles the green, yellow, and red bands known from ZnO, GaN, or  $\text{PbI}_2$ .<sup>[26]</sup>

The emission peaks at 489 nm and 516 nm correspond to the absorption peaks of the low (phase II) and room (phase I) temperature excitonic phases that, as discussed above, are both present at low temperatures. The ratio between the relative intensities from these two excitonic peaks also varies from sample to sample as can be seen from comparing *Figure 3,b*, *3,d* and *3,f*. In the films based on single crystal precursor materials, the lowest-energy exciton emission is the most intense, even at low temperatures where the composition of the material should be dominated by the phase with a higher energy emission (phase II). As the samples are excited at 405 nm ( $\sim 4.05$  mW,  $\sim 1.6 \times 10^{17}$  photon/(s cm<sup>2</sup>)) relaxation and energy transfer takes place before emission. Since the emission from the films prepared from crystals (TF–C) is dominated by the 516 nm exciton emission, the energy is funneled to the remaining parts of the material that are in the high temperature phase, and also to the defect states that are more emissive at low temperature.<sup>[33]</sup> In the films prepared from amorphous powders, both the higher-energy exciton peak and the low-energy defect emission (550–600 nm) are more pronounced than in the TF–C film, compared to the 516 nm exciton emission. This indicates that the concentration of defect states present in these films is higher, but also that the energy transfer to the lower energy exciton state is less efficient. This is in agreement with the small grain size observed in the AFM measurements and illustrates that the quality of the precursor material has pronounced effects on the quality of the deposited films, even if the differences in the X-ray diffraction patterns are negligible at room temperature. This is critical, as in many studies the different emissive transitions are analyzed as strong many-body interactions between the excitons in the

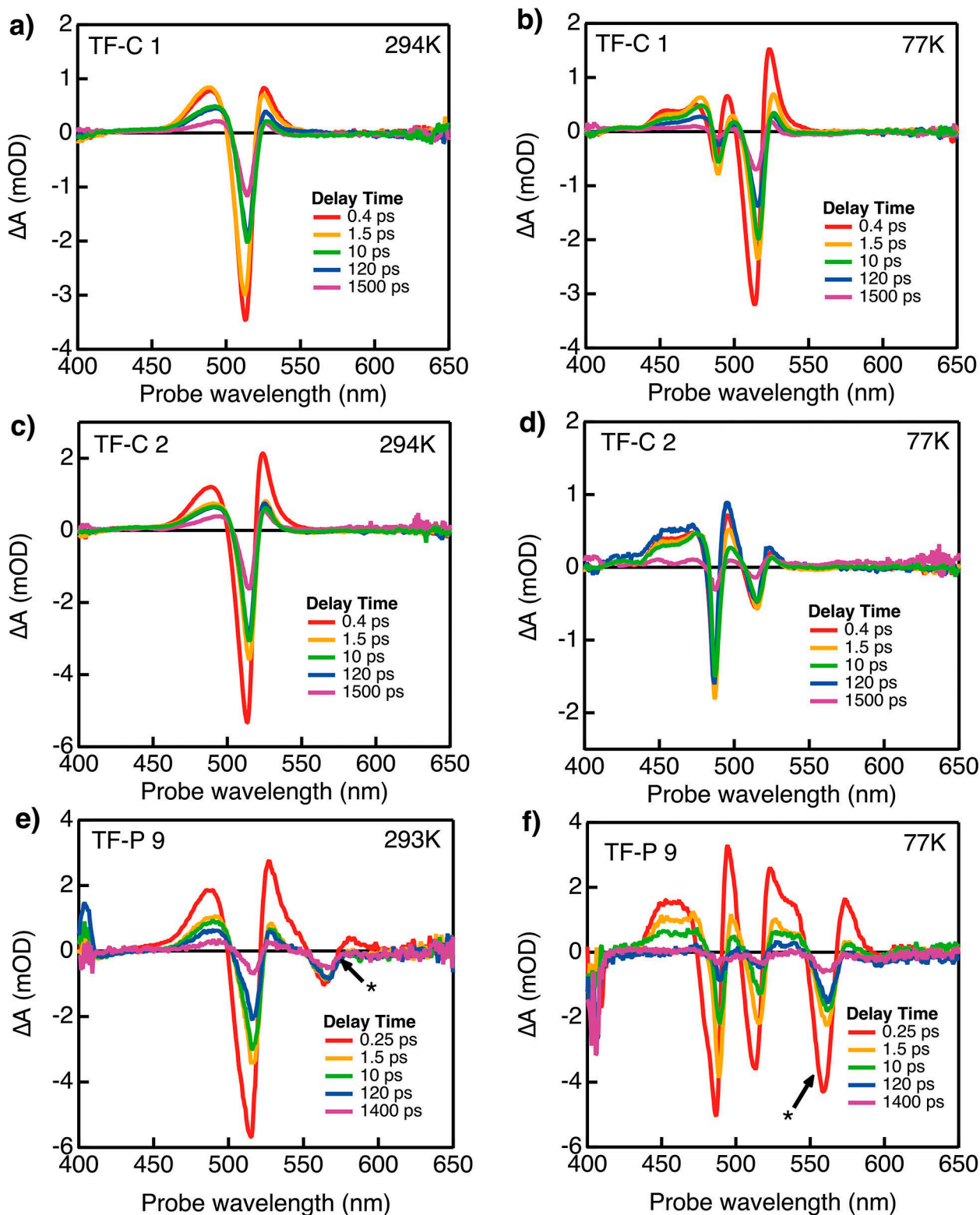


**Figure 3.** Femtosecond transient absorption (TA) experiments on  $\text{BA}_2\text{PbI}_4$  films made from crystalline precursors at 294 K and 77 K as a function of delay times. a), b), c), d) TA Spectra of thin films made from single crystals. e), f) TA Spectra of unoptimized thin films made from powders. Absorbed photon intensities around  $\sim 1.6 \times 10^{12}$  ph/( $\text{cm}^2$  pulse).

inorganic layer which may lead to formation of higher order biexcitons species.<sup>[12,31,34]</sup> In order to further understand the interactions, relaxation and energy transfer processes in the thin films occurring before emission, we measured the changes in absorption due to photoexcitation with an ultrafast transient absorption experiments shown below.

### *Femtosecond Transient Absorption (TA)*

In order to clarify the different relaxation and energy transfer processes occurring between the different energy states in  $\text{BA}_2\text{PbI}_4$  films, we have performed ultrafast transient absorption (TA) measurements as a function of temperature. In these measurements, the films were photoexcited at 405 nm with absorbed photon intensities around  $\sim 1.6 \times 10^{12}$  ph/( $\text{cm}^2$  pulse). We have used a low excitation fluence in order to avoid second order effects due to generation of multiple excitons in a single inorganic slab, see *Figure S3* in the *Supporting Information*. The changes in absorption due to photoexcitation were detected using short broadband pulses obtained from continuum generation in a calcium fluoride ( $\text{CaF}_2$ ) crystal in the range of 450 nm to 800 nm. We measured  $\text{BA}_2\text{PbI}_4$  thin films made from single crystal precursor materials, as they exhibit less emission from extrinsic defect trap states. The TA spectra at room temperature (294 K) for different samples (TF-C 1, TF-C 2) are shown in *Figure 3,a* and *3,c*. At room temperature, the TA spectra exhibit the typical features of 2D perovskites or 2D quantum wells determined in literature: a bleach of the exciton (XB) at  $\sim 512$  nm, corresponding to band-edge filling by photogenerated excitons. There is additional photoinduced absorption (PA) around the main XB which has been attributed to band gap renormalization (BGR) due to exciton–exciton interactions.<sup>[35]</sup> In *Figure 3,b* and *3,d* the TA spectra of  $\text{BA}_2\text{PbI}_4$  films made from crystalline precursor material at 77 K are shown. The TA spectra are more complex than the room temperature spectra and exhibit two bleach features, originating from the exciton transition of the low temperature phase ( $\sim 484$  nm) and the room temperature phase ( $\sim 512$  nm), in addition to photoinduced absorption (PA) around the XB peaks. The relative TA intensities from the different phases (484 nm and  $\sim 512$  nm) vary from sample to sample, even under the exact processing conditions and using the same precursor materials, as evident from comparing the TA spectra in *Figure 3,b* and *3,d* (see more films in *Figure S4* in the *Supporting Information*). For the film TF-C1 in *Figure 3,b*, the exciton features are more

pronounced, while this is reversed for TF-C2 in *Figure 3,d*. These differences are likely a result of variations in the efficiency of energy migration and transfer through the film, which is tightly linked to the crystallinity and morphology. As shown on *Figure 3e*, and *3,f*, the TA spectra of unoptimized films made from powder samples exhibit changes in absorption from the self-trapped exciton defect states at mainly 560 nm, even at room temperature. These observations are consistent with the fluorescence measurements discussed above.

In *Figure 4,a*, the temporal dynamics obtained from the TA measurements on the thin films made from crystals (TF-C) at 77 K from the different wavelengths are shown; the exciton bleach (XB at  $\sim 485$  and  $\sim 512$  nm) and photoinduced absorption (PA at  $\sim 475$  nm, 496 nm and 524 nm). The temporal decay from each of the different observed transitions vary from sample to sample (TF-C1 and TF-C 2). While this complicates the analysis of the data, some clear observation can be made. For both samples, the contribution from the high-energy exciton peak (characterized by the decay of the XB at 487/489 nm in *Figure 4,c*) decays relatively slowly compared to that of the low energy exciton peak ( $\sim 512$  nm). This shows that the photo-physics of these different excitonic states are quite distinct. It also sheds some light on the possible energy transfer from the high-energy to the low-energy exciton states. While there is some funneling from the high- to the low-energy excitons, on the time scales shown in *Figure 4,c*, there does not seem to be a clear transfer, which would result in a faster decay of the high-energy excitons and a slower decay of the low-energy ones. This indicates that energy transfer through the films is not always 100% efficient and shows large sample to sample variation. The likely partial explanation is that different grains of the material go through phase transitions at different temperature. At low temperature, some small grains in the material may stay in the high-temperature phase. However, since transport over grain boundaries is relatively inefficient, some parts of the material are 'isolated' sufficiently from the low energy part to ensure substantial emission from these regions. This behavior is also supported by the photoluminescence measurements discussed above.

The variation related to TA features from the different phases in thin films made from single crystal precursors should be related to the film crystallization on the substrate. From AFM measurements the microstructure of thin films made from crystals consists on grains of  $\sim 600$  nm size (*Figure S2*). However, at low

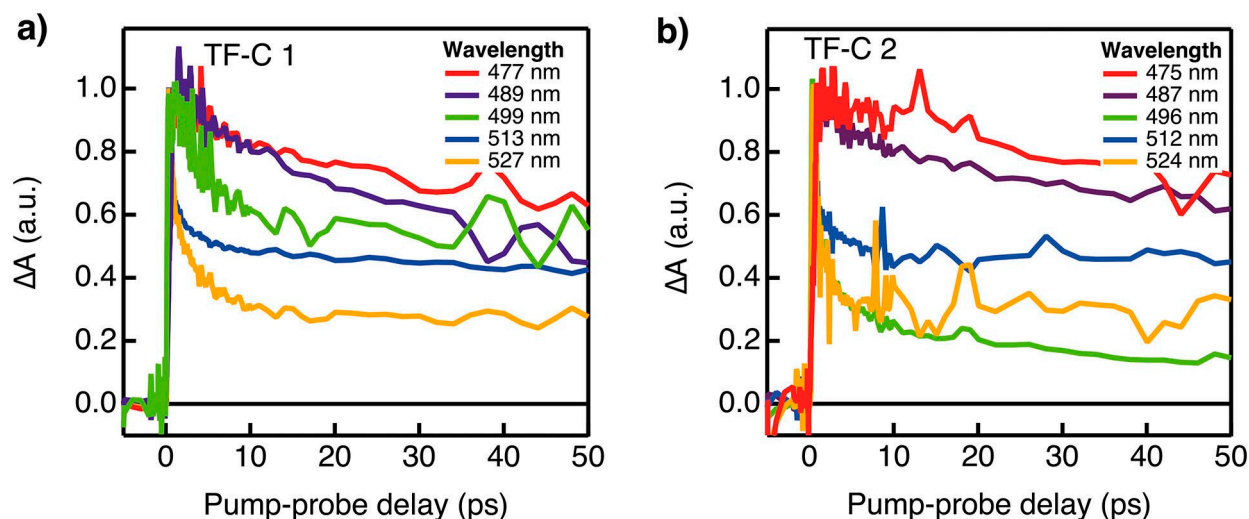


**Figure 4.** Femtosecond transient absorption (TA) experiments on  $\text{BA}_2\text{PbI}_4$  films made from crystalline precursors at 77 K. a), b) Temporal dynamics of different transitions, exciton bleach (XB at  $\sim 485$  and  $\sim 512$  nm) and photoinduced absorption (PA at  $\sim 475$  nm, 496 nm and 524 nm). Absorbed photon intensities around  $\sim 1.6 \times 10^{12}$  ph/( $\text{cm}^2$  pulse).

temperature it is not possible to determine the specific phase (484 nm and  $\sim 512$  nm) in which the grains will be. On the other hand, unoptimized films that are obtained from amorphous powder precursors invariably contain more trap states (bound excitons) that lead to substantial (longer-lived) emission around 560 nm and 600 nm (Figure S1 in the Supporting Information) or even changes in absorption in the TA spectra (Figure 3,e and 3,f). These measurements show that BA-based 2D perovskites are very sensitive to deposition conditions and most of the effects are seen by studying the optoelectronic properties as a function of temperature. This is likely to be the result of the weak interactions between the alkylammonium chains resulting in a relatively soft lattice of 2D structures with alkylammonium chains. This leads to larger dynamic disorder in the inorganic structure and variations in the optoelectronic properties, phase transitions and grain formation. This is important to take into account in previous studies in literature where the interpretation of the exciton bands can be severely affected by the film crystallization and presence of trap states.<sup>[12,18,23,33,36]</sup>

## Conclusions

In this work, it has been examined how the ground state absorption, emission and excited state dynamics of spin coated thin films of  $\text{BA}_2\text{PbI}_4$  are affected by the processing conditions and the nature of the precursor

compounds. Two types of starting material have been evaluated, powders and crystals grown from solution. According to XRD analysis, both precursors are nominally pure high-quality crystalline materials, and spin coating followed by annealing results in 2D perovskite layers, but the powder-based films typically exhibit a low-intensity extra reflection indicating the presence of an impurity phase. While the XRD analysis shows that the samples are very similar, significant differences are observed in the optical properties, depending on the precursor materials and processing conditions. In general, lower quality precursors and unoptimized processing conditions lead to a larger relative intensity emission from broadband self-trapped exciton defect states. This should be considered in the design of broadband perovskite emitters which is often attributed to self-trapped excitons by lattice deformation. In addition, even for high quality samples, differences are observed, especially in the emission intensities from the excitonic phases at low temperature.  $\text{BA}_2\text{PbI}_4$  is known to undergo a phase transition at 253 K, but both the steady state absorption and emission, and the transient absorption measurements on thin films show that the phase transition is not uniform, and the two phases coexist below the phase transition temperature. The presence of the room-temperature phase, even at low temperature, results in significant energy transfer in the excited state, affecting the excited state dynamics and hence the emission properties. These effects show that 2D perovskites with alkyl-chains (BA) have a relatively soft structure due to weak interaction

between the alkyl chains, leading to increased octahedral (dynamic) disorder. This also introduces structural phase transitions and high sensitivity to precursors and processing conditions. These results show that it is difficult to make absolute statements about the optoelectronic properties and excited state dynamics of 2D perovskites with alkylammonium molecules, because the excited state properties are strongly affected by the structural disorder (softness), external impurities and structural defects. Using less flexible ammonium ions in 2D perovskites is expected to lead to more rigid structures that are less affected by such problems.

## Experimental Section

### Starting Materials

All chemicals were purchased from *Sigma–Aldrich* and used as received.

### Synthesis of $BA_2PbI_4$

PbO powder (1 mmol) was dissolved in a mixture of 57% w/w aqueous HI solution (7.6 mmol) and 50% aqueous  $H_3PO_2$  (1.5 mmol) by heating to 393 K under constant magnetic stirring. In a separate beaker, the organic compound, *n*-BA (2 mmol) was neutralized with HI 57% w/w (3.8 mmol) in an ice bath (BA). Then, the organic solution was slowly added to the  $PbI_2$  solution while heating to 393 K. Subsequently, the stirring was stopped, and the solution was left to cool to room temperature precipitating the 2D powders &bk,(~ 2 h)&ek,. The powders were isolated by suction filtration and thoroughly dried under reduced pressure. For  $BA_2PbI_4$  crystals, the starting solutions have ~ 10 mmol of precursors and are cooled slowly (~ 10 K per h) for ~ 2 to 12 h.

### Deposition of Films

Quartz substrates were cleaned by submerging in a vial with a mixture of distilled water and soap, which were then put in a sonic bath at 323 K for 15 min. Afterwards, the quartz substrates were rinsed with distilled water, acetone and propyl ethanol and put in an oven at 373 K for 20 min. Fabrication of the 2D hybrid perovskites layers was carried out in a nitrogen-filled glovebox. Prior to film fabrication, the quartz substrates were treated with oxygen plasma for 2 min. The starting solutions were prepared by dissolving  $BA_2PbI_4$  (0.25 M) in dimethylformamide (DMF) at 343 K

for 2 h. Then, the precursor solution was filtered with a 0.45  $\mu$ m pore size. Films were prepared by spin-coating 100  $\mu$ L of starting fresh solution (ramp 1000 rpm/s, 4000 rpm for 30 s) on the plasma-treated quartz substrate heated at 433 K and subsequently post-annealing it at 373 K for 15 min (hot-casting).<sup>[9]</sup>

### Optical Characterization

Absorption spectra were recorded with a UV/VIS *Perkin-Elmer Lambda 1050* spectrophotometer equipped with an integrated sphere. The films were placed under an angle of 10° inside the sphere to detect the total fraction of reflected and transmitted photons ( $F_{R+T}$ ).

### Temperature Dependent Absorption (% Transmission) and Photoluminescent Measurements

Thin films on quartz substrates were placed in a sealed cryostat under helium flow (temperatures down to 18 K). The absorption was measured with an *Ocean-optics Maya 2000 pro* spectrometer (196 nm to 1120 nm, 100  $\mu$ m slit) coupled with a UV/VIS light source *DH-2000* (halogen lamp). The photoluminescent emission spectra were recorded using an *Oceanoptics flame-s* miniature spectrometer *FLM500719* (350 nm to 1000 nm, grating #03 600/500) coupled with a *Thorlabs* collimated laser diode with a 405 nm excitation wavelength (*CPS405*, Power ~ 4.05 mW,  $A = 0.0482 \text{ cm}^2$ , photon intensity ( $I_0$ ) ~  $1.7 \times 10^{17}$  photons/(s  $\text{cm}^2$ )).

### Femtosecond Transient Absorption (TA) Spectroscopy

Pump-probe transient absorption measurements were performed using a tunable laser system comprising an Yb:KGW laser source (1028 nm) operating at 5 kHz (2.5 kHz repetition rate) with a pulse duration of 180 fs (*PHAROS-SP-06-200*, *Light Conversion*) and an optical parametric amplifier (*ORPHEUS-PO15F5HNP1*, *Light Conversion*). Probe light was generated by continuum generation, focusing a small fraction of the fundamental laser light in a  $CaF_2$  crystal (350 nm to 800 nm). The two-dimensional data was acquired with a transient absorption spectrometer (*HELIOS*, *Ultrafast Systems*). The samples were placed inside a sealed holder and excited at 405 nm with a photon intensity of ~  $3.2 \times 10^{12}$  ph/( $\text{cm}^2$  pulse), and 200  $\mu$ m probe spot size in quasi parallel pump-probe geometry.

## Acknowledgements

This work is funded by the European Research Council Horizon 2020 ERC Grant Agreement no. 648433.

## Author Contribution Statement

S. P. and P.-C. W. prepared and optimized the thin films conditions. M. C. G. R. prepared the crystals, powders and thin films and performed the characterization and optical (absorption, photoluminescence and transient absorption) measurements. K. M. F. performed the atomic force microscopy (AFM) experiments. M. C. G. R. and F. C. G. conceived the idea and wrote the manuscript.

## References

- [1] D. H. Cao, C. C. Stoumpos, O. K. Farha, J. T. Hupp, M. G. Kanatzidis, '2D Homologous Perovskites as Light-Absorbing Materials for Solar Cell Applications', *J. Am. Chem. Soc.* **2015**, *137*, 7843–7850.
- [2] C. C. Stoumpos, D. H. Cao, D. J. Clark, J. Young, J. M. Rondinelli, J. I. Jang, J. T. Hupp, M. G. Kanatzidis, 'Ruddlesden–Popper Hybrid Lead Iodide Perovskite 2D Homologous Semiconductors', *Chem. Mater.* **2016**, *28*, 2852–2867.
- [3] H. Tsai, W. Nie, J.-C. Blancon, C. C. Stoumpos, R. Asadpour, B. Harutyunyan, A. J. Neukirch, R. Verduzco, J. J. Crochet, S. Tretiak, L. Pedesseau, J. Even, M. A. Alam, G. Gupta, J. Lou, P. M. Ajayan, M. J. Bedzyk, M. G. Kanatzidis, A. D. Mohite, 'High-efficiency two-dimensional Ruddlesden–Popper perovskite solar cells', *Nature* **2016**, *536*, 312–317.
- [4] M. Yuan, L. N. Quan, R. Comin, G. Walters, R. Sabatini, O. Voznyy, S. Hoogland, Y. Zhao, E. M. Bearegard, P. Kanjanaboos, Z. Lu, D. H. Kim, E. H. Sargent, 'Perovskite energy funnels for efficient light-emitting diodes', *Nat. Nanotechnol.* **2016**, *11*, 872–877.
- [5] R. L. Milot, R. J. Sutton, G. E. Eperon, A. A. Haghighirad, J. M. Hardigree, L. Miranda, H. J. Snaith, M. B. Johnston, L. M. Herz, 'Charge-Carrier Dynamics in 2D Hybrid Metal–Halide Perovskites', *Nano Lett.* **2016**, *16*, 7001–7007.
- [6] O. Yaffe, A. Chernikov, Z. M. Norman, Y. Zhong, A. Velauthapillai, A. Van Der Zande, J. S. Owen, T. F. Heinz, 'Excitons in ultrathin organic-inorganic perovskite crystals', *Phys. Rev. B* **2015**, *92*, 045414.
- [7] G. Lanty, K. Jemli, Y. Wei, J. Leymarie, J. Even, J.-S. Lauret, E. Deleporte, 'Room-Temperature Optical Tunability and Inhomogeneous Broadening in 2D-Layered Organic–Inorganic Perovskite Pseudobinary Alloys', *J. Phys. Chem. Lett.* **2014**, *5*, 3958–3963.
- [8] J.-C. Blancon, A. V. Stier, H. Tsai, W. Nie, C. C. Stoumpos, B. Traoré, L. Pedesseau, M. Kepenekian, F. Katsutani, G. T. Noe, J. Kono, S. Tretiak, S. A. Crooker, C. Katan, M. G. Kanatzidis, J. J. Crochet, J. Even, A. D. Mohite, 'Scaling law for excitons in 2D perovskite quantum wells', *Nat. Commun.* **2018**, *9*, 2254.
- [9] J.-C. Blancon, H. Tsai, W. Nie, C. C. Stoumpos, L. Pedesseau, C. Katan, M. Kepenekian, C. M. M. Soe, K. Appavoo, M. Y. Sfeir, S. Tretiak, P. M. Ajayan, M. G. Kanatzidis, J. Even, J. J. Crochet, A. D. Mohite, 'Extremely efficient internal exciton dissociation through edge states in layered 2D perovskites', *Science* **2017**, *355*, 1288–1292.
- [10] D. B. Mitzi, 'Synthesis, Structure, and Properties of Organic-Inorganic Perovskites and Related Materials', in 'Progress in Inorganic Chemistry', Ed. K. D. Karlin, John Wiley & Sons, 1999, pp. 1–121.
- [11] K. Tanaka, T. Takahashi, T. Kondo, T. Umabayashi, K. Asai, K. Ema, 'Image charge effect on two-dimensional excitons in an inorganic-organic quantum-well crystal', *Phys. Rev. B* **2005**, *71*, 045312.
- [12] T. Ishihara, X. Hong, J. Ding, A. V. Nurmikko, 'Dielectric confinement effect for exciton and biexciton states in Pbl<sub>4</sub>-based two-dimensional semiconductor structures', *Surf. Sci.* **1992**, *267*, 323–326.
- [13] M. C. Gélvez-Rueda, E. M. Hutter, D. H. Cao, N. Renaud, C. C. Stoumpos, J. T. Hupp, T. J. Savenije, M. G. Kanatzidis, F. C. Grozema, 'Interconversion between Free Charges and Bound Excitons in 2D Hybrid Lead Halide Perovskites', *J. Phys. Chem. C* **2017**, *121*, 26566–26574.
- [14] K. Chondroudis, D. B. Mitzi, 'Electroluminescence from an Organic - Inorganic Perovskite Incorporating a Quaterthiophene Dye within Lead Halide Perovskite Layers', *Chem. Mater.* **1999**, *11*, 3028–3030.
- [15] L. Dou, A. B. Wong, Y. Yu, M. Lai, N. Kornienko, S. W. Eaton, A. Fu, C. G. Bischak, J. Ma, T. Ding, N. S. Ginsberg, L.-W. Wang, A. P. Alivisatos, P. Yang, 'Atomically thin two-dimensional organic-inorganic hybrid perovskites', *Science* **2015**, *349*, 1518–1521.
- [16] S. Zhang, C. Yi, N. Wang, Y. Sun, W. Zou, Y. Wei, Y. Cao, Y. Miao, R. Li, Y. Yin, N. Zhao, J. Wang, W. Huang, 'Efficient Red Perovskite Light-Emitting Diodes Based on Solution-Processed Multiple Quantum Wells', *Adv. Mater.* **2017**, *29*, 1606600.
- [17] R. Li, C. Yi, R. Ge, W. Zou, L. Cheng, N. Wang, J. Wang, W. Huang, 'Room-temperature electroluminescence from two-dimensional lead halide perovskites', *Appl. Phys. Lett.* **2016**, *109*, 151101.
- [18] K. Gauthron, J.-S. Lauret, L. Doyennette, G. Lanty, A. Al Choueiry, S. J. Zhang, L. Largeau, O. Mauguin, J. Bloch, E. Deleporte, 'Optical spectroscopy of two-dimensional layered (C<sub>6</sub>H<sub>5</sub>C<sub>2</sub>H<sub>4</sub>-NH<sub>3</sub>)<sub>2</sub>-Pbl<sub>4</sub> perovskite', *Opt. Express* **2010**, *18*, 5912–5919.
- [19] M. Hirasawa, T. Ishihara, T. Goto, K. Uchida, N. Miura, 'Magnetoabsorption of the lowest exciton in perovskite-type compound (CH<sub>3</sub>NH<sub>3</sub>)Pbl<sub>3</sub>', *Phys. B* **1994**, *201*, 427–430.
- [20] D. G. Billing, A. Lemmerer, 'Synthesis, characterization and phase transitions in the inorganic–organic layered perovskite-type hybrids [(C<sub>n</sub>H<sub>2n+1</sub>NH<sub>3</sub>)<sub>2</sub>Pbl<sub>4</sub>], n=4, 5 and 6', *Acta Crystallogr. Sect. B* **2007**, *63*, 735–747.
- [21] T. M. Brenner, D. A. Egger, L. Kronik, G. Hodes, D. Cahen, 'Hybrid organic–inorganic perovskites: low-cost semiconductors with intriguing charge-transport properties', *Nat. Rev. Mater.* **2016**, *1*, 15007.
- [22] C. M. Mauck, W. A. Tisdale, 'Excitons in 2D Organic–Inorganic Halide Perovskites', *Trends Chem.* **2019**, *1*, 380–393.

- [23] T. Ishihara, J. Takahashi, T. Goto, 'Optical properties due to electronic transitions in two-dimensional semiconductors  $(C_nH_{2n+1}NH_3)_2PbI_4$ ', *Phys. Rev. B* **1990**, *42*, 11099.
- [24] F. Thouin, D. A. Valverde-Chávez, C. Quarti, D. Cortecchia, I. Bargigia, D. Beljonne, A. Petrozza, C. Silva, A. Ram, S. Kandada, 'Phonon coherences reveal the polaronic character of excitons in two-dimensional lead halide', *Nat. Mater.* **2019**, *18*, 349–356.
- [25] F. Thouin, S. Neutzner, D. Cortecchia, V. A. Dragomir, C. Soci, T. Salim, Y. M. Lam, R. Leonelli, A. Petrozza, A. R. S. Kandada, C. Silva, 'Stable biexcitons in two-dimensional metal-halide perovskites with strong dynamic lattice disorder', *Phys. Rev. Materials* **2018**, *2*, 034001.
- [26] S. Kahmann, E. K. Tekelenburg, H. Duim, M. E. Kamminga, M. A. Loi, 'Extrinsic nature of the broad photoluminescence in lead iodide-based Ruddlesden–Popper perovskites', *Nat. Commun.* **2020**, *11*, 2344.
- [27] Q. Zhang, Y. Ji, Z. Chen, D. Vella, X. Wang, Q.-H. Xu, Y. Li, G. Eda, 'Controlled Aqueous Synthesis of 2D Hybrid Perovskites with Bright Room-Temperature Long-Lived Luminescence', *J. Phys. Chem. Lett.* **2019**, *10*, 2869–2873.
- [28] H. Duim, S. Adjokatse, S. Kahmann, G. H. ten Brink, M. A. Loi, 'The Impact of Stoichiometry on the Photophysical Properties of Ruddlesden–Popper Perovskites', *Adv. Funct. Mater.* **2020**, *30*, 1907505.
- [29] E. P. Booker, T. H. Thomas, C. Quarti, M. R. Stanton, C. D. Dashwood, A. J. Gillett, J. M. Richter, A. J. Pearson, N. J. L. K. Davis, H. Siringhaus, M. B. Price, N. C. Greenham, D. Beljonne, S. E. Dutton, F. Deschler, 'Formation of Long-Lived Color Centers for Broadband Visible Light Emission in Low-Dimensional Layered Perovskites', *J. Am. Chem. Soc.* **2017**, *139*, 18632–18639.
- [30] D. Cortecchia, S. Neutzner, A. R. S. Kandada, E. Mosconi, D. Meggiolaro, F. D Angelis, C. Soci, A. Petrozza, 'Broadband Emission in Two-Dimensional Hybrid Perovskites: The Role of Structural Deformation', *J. Am. Chem. Soc.* **2017**, *139*, 39–42.
- [31] E. A. Muljarov, S. G. Tikhodeev, N. A. Gippius, T. Ishihara, 'Excitons in self-organized semiconductor/insulator superlattices: Pbl-based perovskite compounds', *Phys. Rev. B* **1995**, *51*, 14370–14378.
- [32] L. Mao, H. Tsai, W. Nie, L. Ma, J. Im, C. C. Stoumpos, C. D. Malliakas, F. Hao, M. R. Wasielewski, A. D. Mohite, M. G. Kanatzidis, 'Role of Organic Counterion in Lead- and Tin-Based Two-Dimensional Semiconducting Iodide Perovskites and Application in Planar Solar Cells', *Chem. Mater.* **2016**, *28*, 7781–7792.
- [33] G. C. Papavassiliou, G. A. Mousdis, C. P. Raptopoulou, A. Terzis, 'Preparation and Characterization of  $[C_6H_5CH_2NH_3]_2PbI_4$ ,  $[C_6H_5CH_2CH_2SC(NH_2)_2]_3PbI_5$  and  $[C_{10}H_7CH_2NH_3]PbI_3$  Organic-Inorganic Hybrid Compounds', *Z. Naturforsch. B* **1999**, *54*, 1405.
- [34] T. Ishihara, 'Optical properties of Pbl-based perovskite structures', *J. Lumin.* **1994**, *60–61*, 269–274.
- [35] Q. Li, T. Lian, 'Ultrafast Charge Separation in Two-Dimensional  $CsPbBr_3$  Perovskite Nanoplatelets', *J. Phys. Chem. Lett.* **2019**, *10*, 566–573.
- [36] N. Kitazawa, M. Aono, Y. Watanabe, 'Temperature-dependent time-resolved photoluminescence of  $(C_6H_5C_2H_4NH_3)_2PbX_4$  (X=Br and I) Absorbance', *Mater. Chem. Phys.* **2012**, *134*, 875–880.

Received June 11, 2020

Accepted July 29, 2020